

Short Communication

# Investigation of Growth kinetics of the Electrochemical Germanium Nanowire Array Deposition in Galvanostatic Regime Using Indium Nanoparticles

Ilya Gavrilin\*, Irina Martynova, Andrei Zakharov and Sergey Gavrilov

National Research University of Electronic Technology (MIET), Bld. 1, Shokin Square, 124498, Zelenograd, Moscow, Russian Federation

\*E-mail: [gavrilin.ilya@gmail.com](mailto:gavrilin.ilya@gmail.com)

Received: 1 December 2021 / Accepted: 6 January 2022 / Published: 2 February 2022

---

The features of growth kinetics of the electrochemical Ge nanowires deposition from GeO<sub>2</sub> aqueous solutions using indium nanoparticles as crystallization centers are reported. The use of the galvanostatic regime makes it possible to identify sections on the obtained potential-time curves that corresponds to the beginning and completion of the Ge nanowires growth process. It has been established that the Ge nanowires formation efficiency does not depend on the indium mass deposited on the substrate. However, the increase of current density leads to a decrease of the indium mass which participates in the Ge nanowires formation.

---

**Keywords:** Ge nanowires, galvanostatic regime, cathodic deposition, nanoparticles.

## 1. INTRODUCTION

Germanium (Ge) nanowires have attracted much attention due to their optical and electrophysical properties [1]. It has been demonstrated that Ge nanowires may be used in metal-ion batteries [2-5], photodetectors [6] and thermoelectricity [7].

Usually, Ge nanowires fabricate by vapor deposition through the vapor-liquid-solid (VLS) mechanism [8-10]. However, VLS methods are highly energy-consuming, technologically complex, toxic and flammable gases are also commonly used in the process (monogerman and hydrogen). Such methods require high temperatures, which limits the range of substrates used for electrodes.

Electrochemical methods for obtaining germanium nanostructures are also known. It is known, that the electrodeposition of germanium from aqueous solution, in practice, the growth is restricted to a few monolayers due to the competing reduction of water to hydrogen gas [11-13]. The use of ionic liquids [14] or melted germanium salts [15] makes it possible to obtain films with thickness greater

than several monolayers. However, the formation of Ge nanowires from non-aqueous electrolytes requires the use of polycarbonate membranes, or ordered porous matrices, for example, porous anodic alumina [16].

Several years ago, the possibility of Ge nanowires synthesis at temperatures below 100°C by electrochemical method from germanium (IV) oxide (GeO<sub>2</sub>) aqueous solutions has been demonstrated. A feature of this method is the use of metal with low melting point (mercury, gallium, indium) as a medium for the dissolution and crystallization of Ge [17-22].

In the study, for the first time the features of galvanostatic cathodic germanium nanowires formation in aqueous solution using indium nanoparticles as the centers of Ge crystallization have been researched.

## 2. EXPERIMENTAL

### 2.1. Preparation of samples

Polished single-crystal p-type silicon wafers with a resistivity of 10 Ω•cm covered with 100 nm thick titanium films and indium nanoparticle arrays have been utilized as substrates for electrochemical deposition. The titanium film has been deposited by magnetron sputtering. Indium nanoparticles have been formed by the vacuum-thermal evaporation of indium pieces (1.8 mg, 5.5 mg, 9.2 mg and 18,4 mg) from a molybdenum evaporator at a residual pressure of  $1 \times 10^{-5}$  Torr, placed at a distance of 40 cm from the substrate. After depositing the metals, the samples have been annealed in a vacuum at 150°C for 10 min [23].

The mass of deposited indium has been determined by the gravimetric method on a Mettler Toledo XP 205 analytical balance ( $d = 0.01$  mg).

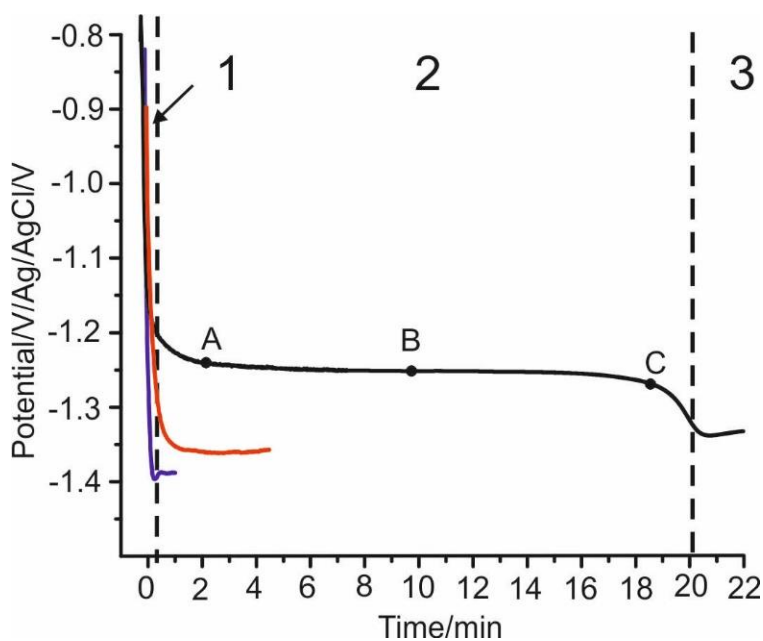
The electrochemical deposition has been performed in a three-electrode cell. A 1x2 cm platinum plate has been served as a counter electrode. A standard electrode (Pt|Ag|AgCl|KCl<sup>-</sup>, Mettler-Toledo InLab Reference Flow) has been used as the reference electrode. The solution has been contained 0.05M GeO<sub>2</sub>, 0.5M K<sub>2</sub>SO<sub>4</sub> and 0.5M C<sub>4</sub>H<sub>6</sub>O<sub>4</sub>. The solution temperature has been controlled using a Termex VT-01 thermostat. The deposition has been performed at a different current density (-0.1 mA/cm<sup>2</sup>; -0.2 mA/cm<sup>2</sup>; -0.5 mA/cm<sup>2</sup>; -1 mA/cm<sup>2</sup>; -2 mA/cm<sup>2</sup>). The current density has been set using an Elins P-45X potentiostat–galvanostat. The prepared samples have been washed in deionized water and dried in an argon flow.

### 2.2. Characterization of samples

The morphology of obtained samples has been studied by scanning electron microscopy (SEM) methods using an FEI Helios NanoLab 650 electron microscope. The obtained SEM images have been processed and analyzed using Fiji software.

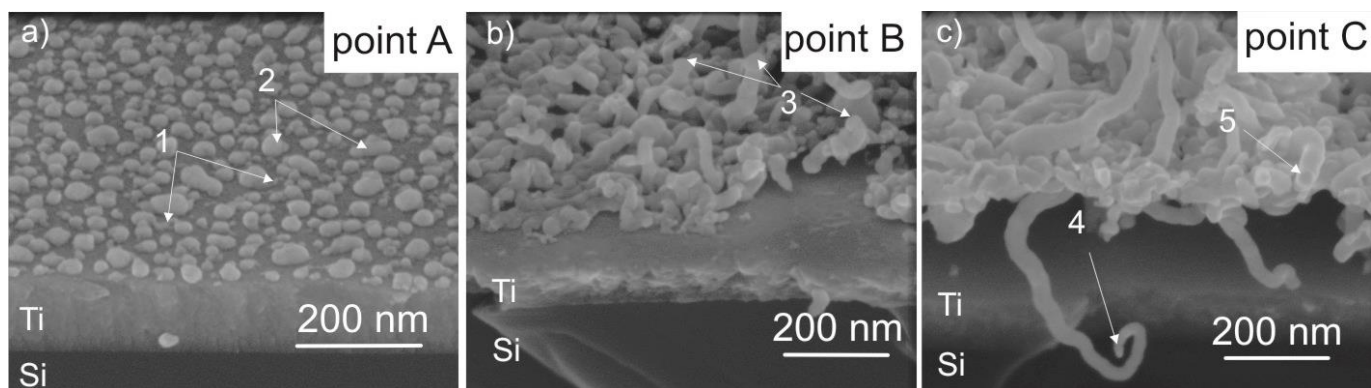
### 3. RESULTS AND DISCUSSION

Fig. 1 shows the potential-time curve recorded during the deposition of germanium on the substrate with indium nanoparticles ( $m_{In} = 3 \mu\text{g}$ ) at a current density  $j = -0.2 \text{ mA/cm}^2$  at a solution temperature of  $20^\circ\text{C}$ .



**Figure 1.** Potential-time curves measured during galvanostatic electrodeposition of Ge at  $-0.2 \text{ mA/cm}^2$  with indium nanoparticles (black curve is the first scan; red curve is the second scan). Blue curve recorded during Ge deposition on titanium foil without indium particles.

The observed form of the potential-time curve indicates the possible occurrence of two cathodic reactions in the electrochemical system [24]. The initial rapid change in the potential characterizes the establishment of equilibrium after the current is applied (region 1 in Fig.1). Region 2 in Fig. 1 is characterized by a slight change in potential from  $-1.25$  to  $-1.4 \text{ V}$  for some time period marked as  $t_{Ge}$ . In this period, a black film is visually observed on the electrode surface. On region 3, a potential of  $-1.54 \text{ V}$  is established and hydrogen gas evolution is observed, which is also observed visually during the experiment. After some time, the formation of gas leads to the flaking of the black film. When the Ge deposition process is repeated on the same sample (before peeling off the black film), a section with a potential of about  $-1.35 \text{ V}$  is observed on the potential-time curve (red curve in Fig.1), and only the formation of gas bubbles is visually observed. For comparison, the potential-time curve (blue curve in Fig.1) has been recorded during the deposition of germanium on the surface of a titanium film without indium nanoparticles. In this case, the potential of the electrode is set at  $-1.4 \text{ V}$  and the formation of gas bubbles is visually observed without the formation of any film. SEM images of the samples at different process times corresponding to points A, B, C in region 2 (Fig. 1) have been presented in Fig. 2.



**Figure 2.** SEM images of the obtained Ge nanowires at different process durations corresponded to the points A, B, C at the potential-time curve (region 2): a - point A, b - point B, c - point C.

According to SEM data (Fig. 2), during the time corresponding to point A on the potential-time curve, the Ge nanowires formation has begun (Fig. 2a - points 1 and 2). On the top of formed Ge nanowires particles of spherical shape (Fig. 2b - point 3) are located. With the process time increasing, the length of the nanowires increases, and the nucleation particle size decreases (Fig. 2b and 2c). This indicates the consumption of the indium during the formation of Ge nanowires, namely, indium dissolution in germanium during the growth of the nanowires, as evidenced by the results of energy dispersive X-ray (EDX) analysis in [3].

Thus, based on the obtained results, it can be concluded that the formation of Ge nanowires corresponds to region 2 on the potential-time curve.

To verify the possibility of using Faraday's law to calculate the current efficiency ( $\eta$ ) of the germanium reduction reaction during the process under consideration, firstly, it is necessary to reveal the dependence behavior of total charge that has passed through region 2 (Fig.1) from the indium mass deposited on the substrate.

To obtain such dependence, the Ge nanowires growth process have been performed using indium nanoparticles of different sizes and mass deposited on the substrates. The results describing the samples have been collected in Table 1.

**Table 1.** The indium nanoparticle arrays parameters from the mass of evaporated indium pieces

No	Indium mass evaporated, mg	Indium mass deposited on a substrate, $\mu\text{g}$ per $1\text{ cm}^2$	Indium nanoparticles mean size, nm
Sample 1	1.8	0.4	4-5
Sample 2	5.5	1.7	9-12
Sample 3	9.2	3	15-18
Sample 4	18.4	6	27-30

Fig. 3 shows the potential-time curves recorded during the deposition of germanium with the different indium mass deposited on a substrate at a current density  $j = -0.2\text{ mA/cm}^2$ .

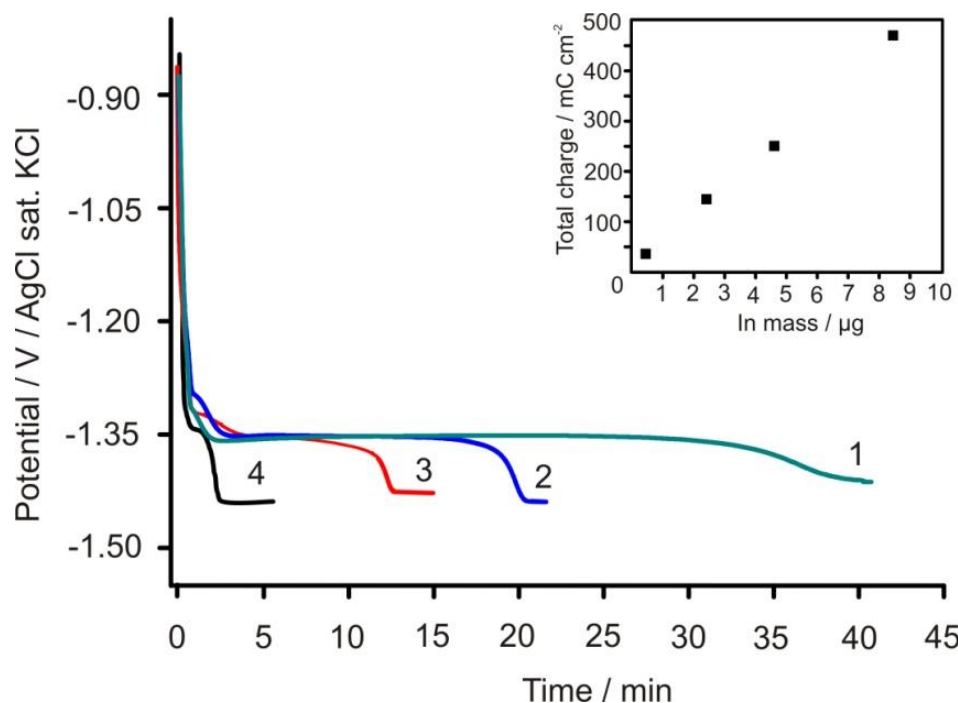


**Figure 3.** Potential-time curves measured during galvanostatic electrodeposition of germanium at  $-0.2 \text{ mA/cm}^2$  using the substrates with different amounts of deposited indium: 1 -  $0.4 \mu\text{g}$ ; 2 -  $1.7 \mu\text{g}$ ; 3 -  $3 \mu\text{g}$ ; 4 -  $6 \mu\text{g}$ . Inset represents dependence of total charge that has passed through region 2 on the mass of indium deposited on the substrate.

The inset shows a directly proportional dependence of the total charge that has passed through region 2 from the mass of indium deposited on the substrate. In this case, efficiency of the Ge nanowires deposition process will be determined by the current efficiency ( $\eta$ ) of the germanium reduction reaction:

$$\eta = \frac{Q_{Ge}}{Q_{total}} \quad (1)$$

, where  $Q_{Ge}$  is the charge expended on the germanium reduction reaction and  $Q_{total}$  is the total charge passing through the system during region 2.

$Q_{Ge}$  is determined from the Faraday's law by the equation:

$$Q_{Ge} = m_{Ge} \cdot \frac{Fz}{M_{Ge}} \quad (2)$$

, where  $M_{Ge}$  is the molar mass of germanium,  $F$  is the Faraday constant, and  $z$  is the number of electrons participating in the reaction, in the case of germanium reduction from the  $\text{GeO}_2$  (IV) aqueous solution  $z=4$  [25].

With the known ratio of indium atoms to germanium atoms  $N_{In}/N_{Ge}=k$ , the dependence of  $Q_{Ge}$  from the mass of indium ( $m_{In}$ ) participating in the formation of Ge nanowires can be presented in the following form:

$$Q_{Ge} = \frac{m_{In}}{k} \cdot \frac{Fz}{M_{In}} \quad (3)$$

, where  $M_{In}$  is the molar mass of indium.

Based on the equations (1) and (3), the current efficiency of the germanium cathodic reduction reaction through the mass of dissolved indium in germanium can be expressed as:

$$\eta = \frac{m_{In}}{kQ_{total}} \frac{Fz}{M_{In}} \quad (4)$$

According to Fig. 3 and coefficient  $k$  (determined from our previous work [3]), the efficiency of the formation of germanium ( $\eta$ ) is  $\sim 0.8$  and stays the same regardless of the indium mass value and the particle size. This efficiency is similar to the value we have obtained using gravimetric measurements. The obtained efficiency is less than 1, which indicates that the reduction of germanium at a given current density is accompanied by parallel electrochemical reactions. Presumably, the primary competition for faradaic efficiency was  $H^+$  reduction at the electrolyte/In interface and at the electrolyte/ $Ge^0$  interface.

In turn, with the simultaneous proceeding of two electrode processes with the different potentials, an increase in the current density can lead to a decrease in the current efficiency of the reaction with a more positive potential [26], in the considered case it is the reaction of  $Ge^0$  production. However, the decrease in the total charge  $Q_{total}$  in region 2 observed in Fig. 4 indicates an increase in the current efficiency of germanium reduction reaction (expression 4).

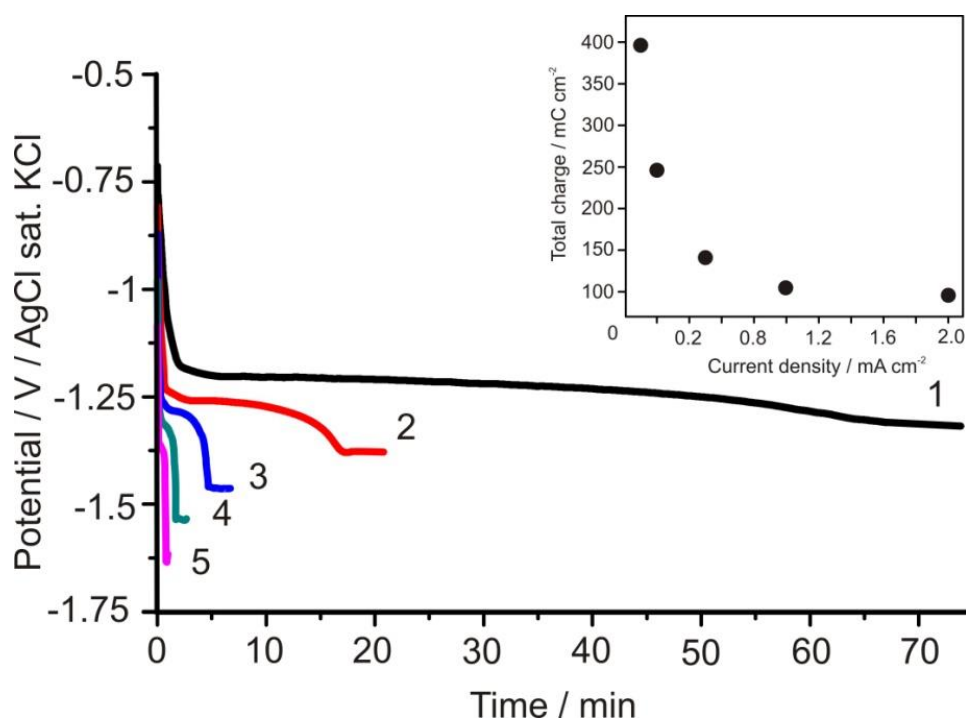


**Figure 4.** Potential-time curves measured during galvanostatic electrodeposition of Ge at the different current density values: 1 – 0.1 mA/cm<sup>2</sup>; 2 - 0.2 mA/cm<sup>2</sup>; 3 - 0.5 mA/cm<sup>2</sup>; 4–1 mA/cm<sup>2</sup>; 5–2 mA/cm<sup>2</sup> at  $m_{In} = 3 \mu\text{g}$ . Inset represents dependence of total charge that has passed through region 2 on the current density.

As  $Q_{total}$  decreases under higher current density values (see the inset in Fig.4), from the equation (4), such behavior suggests that the ratio of the indium particles total mass participated in the Ge nanowires formation process to the indium total mass deposited on the substrate decreases. Also, in our previous work [3] it has been found that with an increase in the current density, the concentration of indium in Ge nanowires increases. It means, that the indium nanoparticle is consumed faster during

the growth of Ge nanowires. In other words, the coefficient  $k$  depends on the current density of the process.

#### 4. CONCLUSION

The features of growth kinetics of the electrochemical Ge nanowires deposition from GeO<sub>2</sub> aqueous solutions using indium particles as crystallization centers are reported for the first time. The use of a galvanostatic regime made it possible to identify the areas on the potential-time curves that corresponded to the beginning and completion of the Ge nanowires growth process. The efficiency of the formation of Ge nanowires has been estimated on the basis of Faraday's law and experimentally determined by EDX analysis of the indium content in germanium. It has been established that the efficiency of the formation of Ge nanowires does not depend on the indium mass deposited on the substrate. In turn, an increase of the current density may lead to a decrease in the mass of indium, which participates in the Ge nanowires formation process.

#### FUNDING

The work was supported by the Grant of the President of the Russian Federation №MK 5839.2021.1.3 and by the Russian Science Foundation.

#### CONFLICT OF INTERESTS

The authors declare no conflicts of interest.

#### References

1. C. Claeys, E. Simoen, Germanium-Based Technologies From Materials to Devices, 1st ed.; Elsevier, New York, 2007, p. 480.
2. T. Kennedy, M. Brandon and K. M. Ryan, *Adv. Mater.*, 28 (2016) 5696.
3. I.M. Gavrilin, Y.O. Kudryashova, A.A. Kuz'mina, T.L. Kulova, A.M. Skundin V.V. Emets, R.L. Volkov, A.A. Dronov, N.I. Borgardt and S.A. Gavrilov, *Journal of Electroanalytical Chemistry*, 8881 (2021) 115209.
4. T.L. Kulova, I.M. Gavrilin, Y.O. Kudryashova and A.M. Skundin, *Mendeleev Communications*, 30 (2020) 775.
5. I.M. Gavrilin, V.A. Smolyaninov, A.A. Dronov, S.A. Gavrilov, A.Yu. Trifonov, T.L. Kulova, A.A. Kuz'mina and A.M. Skundin, *Mendeleev Communications*, 28 (2018) 659.
6. P. Chaisakul, D. Marris-Morini, J. Frigerio, D. Chrastina, M. S. Rouifed, S. Cecchi and L. Vivien, *Nat. Photonics*, 8 (2014) 482.
7. P. N. Martin, Z. Aksamija, E. Pop and U. Ravaioli, *Nano Letters*, 10 (2010) 1120.
8. C. O'Regan, S. Biswas, N. Petkov and J. D. Holmes, *J. Mater. Chem. C*, 2 (2014) 14.
9. G. Collins, M. Kolesnik, V. Krstic and J. D. Holmes, *Chem. Mater.*, 22 (2010) 5235.
10. S. A. Dayeh and S. T. Picraux, *Nano Letters*, 10 (2010) 4032.
11. J. I. Hall and A. E. Koenig, *Trans. Electrochem. Soc.*, 65 (1934) 215.
12. G. Szekeley, *J. Electrochem. Soc.*, 98 (1951) 318.
13. X. Liang, N. Jayaraju and J. L. Stickney, *ECS Trans.*, 11 (2007) 249.

14. A. Lahiri, G. Pulletikurthi, S. Zein El Abedin, F. Endres, *Journal of Solid State Electrochemistry* 19 (2015) 785.
15. N. Chandrasekharan and S. C. Sevov, *J. Electrochem. Soc.*, 157 (2010) C140.
16. R. Al-Salman, J. Mallet, M. Molinari, P. Fricoteaux, F. Martineau, M. Troyon, S. Zein El Abedin and F. Endres, *Phys. Chem. Chem. Phys.*, 10 (2008) 6233.
17. A. I. Carim, S. M. Collins, J. M. Foley and S. Maldonado, *J. Am. Chem. Soc.*, 133 (2011) 13292.
18. J. Gu, S. M. Collins, A. I. Carim, X. Hao, B. M. Bartlett and S. Maldonado, *Nano Letters*, 12 (2012) 4617.
19. L. Ma, J. Gu, E. Fahrenkrug and S. Maldonado, *J. Electrochem. Soc.*, 161 (2014) D3044.
20. N. K. Mahenderkar, Y.-C. Liu, J. A. Koza and J. A. Switzer, *ACS Nano*, 8 (2014) 9524.
21. E. Fahrenkrug and S. Maldonado, *Acc. Chem. Res.*, 48 (2015), 1881.
22. J. DeMuth, E. Fahrenkrug and S. Maldonado, *Solvent Crystal Growth & Design*, 16 (2016) 7130.
23. S. A. Gavrilov, A. A. Dronov, I. M. Gavrilin, R. L. Volkov, N. I. Borgardt, A. Yu. Trifonov, A. V. Pavlikov, P.A. Forsh and P.K. Kashkarov, *Journal of Raman Spectroscopy*, 49 (2018) 810.
24. D. D. Macdonald, *Chronopotentiometry In: Transient Techniques in Electrochemistry*, Springer, 1977, p. 65.
25. B. Lovrecek and J. O. M. Bockris, *The Journal of Physical Chemistry*, 63 (1959) 1368.
26. K. J. Vetter, *Electrochemical Kinetics*, Elsevier, 1967, p. 486.

© 2022 The Authors. Published by ESG ([www.electrochemsci.org](http://www.electrochemsci.org)). This article is an open access article distributed under the terms and conditions of the Creative Commons Attribution license (<http://creativecommons.org/licenses/by/4.0/>).